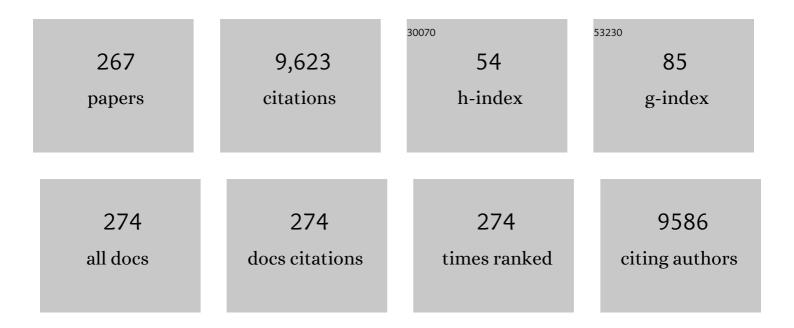
Daniel Guay

List of Publications by Year in descending order

Source: https://exaly.com/author-pdf/27801/publications.pdf Version: 2024-02-01



DANIEL CHAY

#	Article	IF	CITATIONS
1	Defective Metal–Organic Framework-808@Polyaniline Composite Materials for High Capacitance Retention Supercapacitor Electrodes. ACS Applied Energy Materials, 2022, 5, 1235-1243.	5.1	24
2	Au(001) Thin Films: Impact of Structure and Mosaicity on the Oxygen Reduction Reaction in Alkaline Medium. ACS Catalysis, 2022, 12, 1664-1676.	11.2	1
3	Highly porous scaffolds for Ru-based microsupercapacitor electrodes using hydrogen bubble templated electrodeposition. Energy Storage Materials, 2022, 47, 134-140.	18.0	10
4	Impact of Density on the Behavior of Suspension Plasma-Sprayed TiB2 Coatings in the Presence of Molten Aluminum. Journal of Thermal Spray Technology, 2022, 31, 1499-1507.	3.1	2
5	The effect of bond coat on the high-temperature behavior of HVOF-sprayed (Co,Ni)O coating on Cu-Ni-Fe anodes. Surface and Coatings Technology, 2022, 441, 128576.	4.8	4
6	Uncovering Activity-Stability Relationships in Mixed Ir-Based Catalysts Toward Improved Water Electrolysis. ECS Meeting Abstracts, 2022, MA2022-01, 1373-1373.	0.0	0
7	Porous RuO _{<i>x</i>} N _{<i>y</i>} S _{<i>z</i>} Electrodes for Microsupercapacitors and Microbatteries with Enhanced Areal Performance. ACS Energy Letters, 2021, 6, 131-139.	17.4	19
8	Electrodeposited TiB ₂ on graphite as wettable cathode for Al production. Journal of the American Ceramic Society, 2021, 104, 1247-1254.	3.8	6
9	TiB2 Deposited on Graphite by Suspension Plasma Spray as Al Wettable Cathode. Journal of Thermal Spray Technology, 2021, 30, 1535-1543.	3.1	7
10	High-temperature behaviour of HVOF (Co,Ni)O coated Cu-Ni-Fe anodes. Corrosion Science, 2021, 189, 109563.	6.6	7
11	Effect of IrO ₆ Octahedron Distortion on the OER Activity at (100) IrO ₂ Thin Film. ACS Catalysis, 2020, 10, 806-817.	11.2	52
12	Sampled current voltammetry for kinetic studies on materials unsuitable for rotating discs or microelectrodes: Application to the oxygen reduction reaction in acidic medium. Electrochimica Acta, 2020, 362, 136946.	5.2	8
13	Understanding the Improved Activity of Dendritic Sn1Pb3 Alloy for the CO2 Electrochemical Reduction: A Computational–Experimental Investigation. ACS Catalysis, 2020, 10, 10726-10734.	11.2	11
14	Rethinking Pseudocapacitance: A Way to Harness Charge Storage of Crystalline RuO ₂ . ACS Applied Energy Materials, 2020, 3, 4144-4148.	5.1	11
15	OER Performances of Cationic Substituted (100)-Oriented IrO ₂ Thin Films: A Joint Experimental and Theoretical Study. ACS Applied Energy Materials, 2020, 3, 5229-5237.	5.1	14
16	Progress in the electrochemical reduction of CO2 on hierarchical dendritic metal electrodes. Current Opinion in Electrochemistry, 2020, 23, 145-153.	4.8	6
17	Suspension plasma spray deposition of CoxNi1-xO coatings. Surface and Coatings Technology, 2020, 399, 126168.	4.8	8
18	High Areal Capacity Porous Sn-Au Alloys with Long Cycle Life for Li-ion Microbatteries. Scientific Reports, 2020, 10, 10405.	3.3	9

#	Article	IF	CITATIONS
19	Cold-Sprayed Cu-Ni-Fe Anodes for CO2-Free Aluminum Production. Journal of Thermal Spray Technology, 2020, 29, 670-683.	3.1	7
20	Uncovering the nature of electroactive sites in nano architectured dendritic Bi for highly efficient CO2 electroreduction to formate. Applied Catalysis B: Environmental, 2020, 274, 119031.	20.2	46
21	Double Approach Towards 3D Electrodeposited RuOx Porous Structure for High Energy/High Power Micro-Supercapacitors. ECS Meeting Abstracts, 2020, MA2020-01, 2828-2828.	0.0	0
22	Study of Li Metal/C Paper Electrodes for Li/S Batteries By Operando Dilatometry. ECS Meeting Abstracts, 2020, MA2020-01, 561-561.	0.0	0
23	Regeneration of Reactive Pd Surfaces in Au-Pd Nanoparticles after Electrochemical Aging. ECS Meeting Abstracts, 2020, MA2020-01, 2665-2665.	0.0	Ο
24	CO2 Reduction to Formate on Amine Modified Pb Electrodes. ECS Meeting Abstracts, 2020, MA2020-01, 1519-1519.	0.0	0
25	A Computational-Experimental Investigation of the Mechanisms Responsible for the Enhanced CO2 Electrochemical Reduction of Dendritic Sn1Pb3 Alloy. ECS Meeting Abstracts, 2020, MA2020-01, 2630-2630.	0.0	1
26	Synthesis and Characterization of (Co,Ni)O Solid Solutions As Protective Coatings for Inert Anodes in Aluminum Electrolysis. ECS Meeting Abstracts, 2020, MA2020-01, 1252-1252.	0.0	0
27	(Co,Ni)O Coated Anodes for CO2-Free Al Production. ECS Meeting Abstracts, 2020, MA2020-01, 2911-2911.	0.0	0
28	TiB2-Coated Graphite As Wettable Cathode for Al Production. ECS Meeting Abstracts, 2020, MA2020-01, 1253-1253.	0.0	0
29	Model Operational Matrix for the Betterment of Ruthenium As a Catalyst for the Electrochemical Nitrogen Reduction Reaction to Ammonia in Aqueous Electrolytes. ECS Meeting Abstracts, 2020, MA2020-01, 1809-1809.	0.0	0
30	Domain Size Dependence of the Oxygen Reduction Reaction on (100)-Oriented Au Thin Films. ECS Meeting Abstracts, 2020, MA2020-01, 2670-2670.	0.0	0
31	Ir Decorated Fractal Ni Catalysts for the Oxygen Evolution Reaction. ECS Meeting Abstracts, 2020, MA2020-01, 1538-1538.	0.0	Ο
32	Electrodeposited TiB2 Coating on Graphite As Wettable Cathode for Al Production. ECS Meeting Abstracts, 2020, MA2020-01, 1244-1244.	0.0	0
33	Evaluation of Porous Ni(Zn) Materials As 3D Matrices for Li Metal Electrodes. ECS Meeting Abstracts, 2020, MA2020-01, 2842-2842.	0.0	Ο
34	Study of Li Metal/C Paper Electrodes for Li/S Batteries By Operando Dilatometry. ECS Meeting Abstracts, 2020, MA2020-02, 3778-3778.	0.0	0
35	Synthesis and Characterization of (Co,Ni)O Solid Solutions As Protective Coatings for Inert Anodes in Aluminum Electrolysis. ECS Meeting Abstracts, 2020, MA2020-02, 3759-3759.	0.0	0
36	Double Approach Towards 3D Electrodeposited RuOx Porous Structure for High Energy/High Power Micro-Supercapacitors. ECS Meeting Abstracts, 2020, MA2020-02, 3801-3801.	0.0	0

#	Article	IF	CITATIONS
37	Metal–Organic-Frameworks-Derived Cu/Cu ₂ O Catalyst with Ultrahigh Current Density for Continuous-Flow CO ₂ Electroreduction. ACS Sustainable Chemistry and Engineering, 2019, 7, 15739-15746.	6.7	39
38	Hydrogen Bubble Templating of Fractal Ni Catalysts for Water Oxidation in Alkaline Media. ACS Applied Energy Materials, 2019, 2, 5734-5743.	5.1	20
39	Study of Cu-Ni-Fe Alloys as Inert Anodes for Al Production in Low-Temperature KF-AlF3 Electrolyte. Metallurgical and Materials Transactions B: Process Metallurgy and Materials Processing Science, 2019, 50, 3103-3111.	2.1	14
40	3D Interdigitated Microsupercapacitors with Record Areal Cell Capacitance. Small, 2019, 15, 1901224.	10.0	27
41	Electroreduction of CO ₂ to formate on amine modified Pb electrodes. Journal of Materials Chemistry A, 2019, 7, 11272-11281.	10.3	55
42	Synthesis and thermal stability of (Co,Ni)O solid solutions. Journal of the American Ceramic Society, 2019, 102, 5063-5070.	3.8	8
43	Probing the surface sensitivity of dimethyl ether oxidation on epitaxially-grown PtRh(1 0 0) alloys: Insights into the challenge of improving on Pt(1 0 0). Journal of Catalysis, 2019, 369, 405-414.	6.2	3
44	Vertically Aligned Ni Nanowires as a Platform for Kinetically Limited Water-Splitting Electrocatalysis. Journal of Physical Chemistry C, 2019, 123, 1082-1093.	3.1	5
45	Promotion of Glycerol Oxidation by Selective Ru Decoration of (100) Domains at Nanostructured Pt Electrodes. ChemElectroChem, 2019, 6, 1784-1793.	3.4	6
46	Impact of a post-casting homogenization treatment on the high-temperature oxidation resistance of a Cu-Ni-Fe alloy. Corrosion Science, 2019, 147, 321-329.	6.6	13
47	Tuning Pt–Ir Interactions for NH ₃ Electrocatalysis. ACS Catalysis, 2018, 8, 2508-2518.	11.2	46
48	Enhanced electrocatalytic nitrate reduction by preferentially-oriented (100) PtRh and PtIr alloys: the hidden treasures of the â€~miscibility gap'. Applied Catalysis B: Environmental, 2018, 221, 86-96.	20.2	44
49	Aqueous-phase electrochemical reduction of CO2 based on SnO2CuO nanocomposites with improved catalytic activity and selectivity. Catalysis Today, 2018, 318, 2-9.	4.4	14
50	Hydrazine Electro-Oxidation at Epitaxial Ir Pt100â^' Alloys. , 2018, , 1-8.		0
51	NH3 Oxidation on Well-Defined Surfaces and Proxies of the Same. , 2018, , 752-760.		0
52	Perovskite-Type Catalysts Prepared by Nanocasting: Effect of Metal Silicates on the Electrocatalytic Activity toward Oxygen Evolution and Reduction Reactions. ACS Applied Energy Materials, 2018, 1, 2565-2575.	5.1	7
53	Selective electroreduction of CO 2 to formate on Bi and oxide-derived Bi films. Journal of CO2 Utilization, 2017, 19, 276-283.	6.8	78
54	Pt Thin Films with Nanometer-Sized Terraces of (100) Orientation. Journal of Physical Chemistry C, 2017, 121, 12188-12198.	3.1	8

#	Article	IF	CITATIONS
55	Nanostructured Pt Surfaces with Ir Submonolayers for Enhanced NH ₃ Electroâ€oxidation. ChemElectroChem, 2017, 4, 1327-1333.	3.4	14
56	Hydrogen solubility of bcc PdCu and PdCuAg alloys prepared by mechanical alloying. Journal of Alloys and Compounds, 2017, 698, 725-730.	5.5	14
57	Pt nanostructures with different Rh surface entities: Impact on NH3 electro-oxidation. Journal of Catalysis, 2017, 354, 270-277.	6.2	12
58	Selective electroreduction of CO ₂ to formate on 3D [100] Pb dendrites with nanometer-sized needle-like tips. Journal of Materials Chemistry A, 2017, 5, 20747-20756.	10.3	56
59	The Art of Decoration: Rhodium-Modified Platinum Films with Preferential (100) Orientation as Electrocatalysts for Nitrate Reduction and Dimethyl Ether Oxidation. Journal of Physical Chemistry C, 2017, 121, 15233-15247.	3.1	10
60	Atypical Properties of FIB-Patterned RuO _{<i>x</i>} Nanosupercapacitors. ACS Energy Letters, 2017, 2, 1734-1739.	17.4	25
61	CO2 electroreduction at AuxCu1-x obtained by pulsed laser deposition in O2 atmosphere. Electrochimica Acta, 2017, 246, 115-122.	5.2	18
62	Trends in Catalysis and Catalyst Cost Effectiveness for N ₂ H ₄ Fuel Cells and Sensors: a Rotating Disk Electrode (RDE) Study. Journal of Physical Chemistry C, 2016, 120, 4717-4738.	3.1	51
63	Gold–Manganese Oxide Core–Shell Nanoparticles Produced by Pulsed Laser Ablation in Water. Journal of Physical Chemistry C, 2016, 120, 22635-22645.	3.1	13
64	Interdigitated microelectrodes for oxygen removal in N 2 H 4 sensors. Electrochemistry Communications, 2016, 71, 56-60.	4.7	7
65	Hydrogen Solubility of Magnetron Co-Sputtered FCC and BCC PdCuAu Thin Films. Journal of Physical Chemistry C, 2016, 120, 5297-5307.	3.1	7
66	Identification of Cu surface active sites for a complete nitrate-to-nitrite conversion with nanostructured catalysts. Applied Catalysis B: Environmental, 2016, 187, 399-407.	20.2	48
67	Hydrogen permeability of PdCuAu membranes prepared from mechanically-alloyed powders. Journal of Membrane Science, 2016, 509, 68-82.	8.2	13
68	Mechanically alloyed Cu-Ni-Fe-Y material as inert anode for Al production. Minerals, Metals and Materials Series, 2016, , 1277-1281.	0.4	1
69	Cold Spray deposition of mechanically alloyed Cu-Ni-Fe material for application as inert anodes for aluminum production. Minerals, Metals and Materials Series, 2016, , 1283-1287.	0.4	0
70	3D RuO ₂ Microsupercapacitors with Remarkable Areal Energy. Advanced Materials, 2015, 27, 6625-6629.	21.0	206
71	Electrooxidation of Ammonia at Tuned (100)Pt Surfaces by using Epitaxial Thin Films. ChemElectroChem, 2015, 2, 1187-1198.	3.4	17
72	Formic acid oxidation on antimony-covered platinum films with a preferential (100) orientation. Journal of Power Sources, 2015, 299, 315-323.	7.8	4

#	Article	lF	CITATIONS
73	Preferentially (100) oriented Pt thin film with less than a monolayer of Bi, Pd and Sb adatoms: application for formic acid oxidation. Electrochimica Acta, 2015, 162, 237-244.	5.2	7
74	Dopamine and ascorbic acid electro-oxidation on Au, AuPt and Pt nanoparticles prepared by pulse laser ablation in water. Electrochimica Acta, 2015, 159, 174-183.	5.2	56
75	Mechanistic Similarity in Catalytic N ₂ Production from NH ₃ and NO ₂ [–] at Pt(100) Thin Films: Toward a Universal Catalytic Pathway for Simple N-Containing Species, and Its Application to <i>in Situ</i> Removal of NH ₃ Poisons. Journal of Physical Chemistry C. 2015, 119, 9860-9878.	3.1	40
76	On the key role of Cu on the oxidation behavior of Cu–Ni–Fe based anodes for Al electrolysis. Corrosion Science, 2015, 101, 105-113.	6.6	32
77	Pulsed Laser Deposition of PdCuAu Alloy Membranes for Hydrogen Absorption Study. Journal of Physical Chemistry C, 2015, 119, 26451-26458.	3.1	11
78	Cold sprayed Cu–Ni–Fe anode for Al production. Corrosion Science, 2015, 90, 259-265.	6.6	26
79	Influence of Partial Substitution of Cu by Various Elements in Cu-Ni-Fe Alloys on Their High-Temperature Oxidation Behavior. , 2015, , 1187-1191.		1
80	Outer and Inner Surface Contribution of Manganese Dioxides Energy Storage Characterization by Cavity Microelectrode Technique. ECS Transactions, 2014, 58, 53-59.	0.5	4
81	Transmission line model of mixed ionic and electronic conductor: the case of hydrous ruthenium oxide. Journal of Solid State Electrochemistry, 2014, 18, 2913-2920.	2.5	0
82	Formic acid oxidation on Bi covered Pt electrodeposited thin films: influence of the underlying structure. Electrochimica Acta, 2014, 134, 486-495.	5.2	11
83	High-resolution on-chip supercapacitors with ultra-high scan rate ability. Journal of Materials Chemistry A, 2014, 2, 7170-7174.	10.3	104
84	Highly active PtAu alloy nanoparticle catalysts for the reduction of 4-nitrophenol. Nanoscale, 2014, 6, 2125-2130.	5.6	211
85	Hydrous RuO 2 /carbon nanowalls hierarchical structures for all-solid-state ultrahigh-energy-density micro-supercapacitors. Nano Energy, 2014, 10, 288-294.	16.0	176
86	Kinetically stable Pt x Ir 100-x alloy thin films prepared by pulsed laser deposition: Oxidation of NH 3 and poisoning resistance. Electrochimica Acta, 2014, 142, 289-298.	5.2	16
87	Hydrogen solubility in PdCuAg ternary alloy films prepared by electrodeposition. International Journal of Hydrogen Energy, 2014, 39, 15810-15818.	7.1	9
88	Hydrogen solubility in PdCuAu alloy thin films prepared by electrodeposition. International Journal of Hydrogen Energy, 2014, 39, 3487-3497.	7.1	12
89	Formic acid electro-oxidation at PtAu alloyed nanoparticles synthesized by pulsed laser ablation in liquids. Journal of Power Sources, 2014, 248, 273-282.	7.8	66
90	Structure and valence properties of ceria films synthesized by laser ablation under reducing atmosphere. Materials Research Express, 2014, 1, 015704.	1.6	22

#	Article	IF	CITATIONS
91	Evaluation of a Pre-Oxidation Treatment for Limiting Electrolyte Penetraton in Cu-Ni-Fe Anode during Al Electrolysis. , 2014, , 1305-1307.		1
92	Evaluation of a Pre-Oxidation Treatment for Limiting Electrolyte Penetration in Cu-Ni-Fe Anode during Al Electrolysis. , 2014, , 1305-1307.		0
93	Hydrazine Oxidation at Porous and Preferentially Oriented {100} Pt Thin Films. Electrocatalysis, 2013, 4, 76-84.	3.0	30
94	Consolidation of mechanically alloyed Cu–Ni–Fe material by spark plasma sintering and evaluation as inert anode for aluminum electrolysis. Journal of Alloys and Compounds, 2013, 580, 256-261.	5.5	20
95	Electrodeposited platinum thin films with preferential (100) orientation: Characterization and electrocatalytic properties for ammonia and formic acidÂoxidation. Journal of Power Sources, 2013, 225, 323-329.	7.8	52
96	Measurements of hydrogen solubility in CuxPd100â^'x thin films. Electrochimica Acta, 2013, 90, 615-622.	5.2	31
97	Influence of the configuration in planar interdigitated electrochemical micro-capacitors. Journal of Power Sources, 2013, 230, 230-235.	7.8	88
98	Measurement of Hydrogen Solubility in Pd _{<i>x</i>} Cu _{100–<i>x</i>} Thin Films Prepared by Pulsed Laser Deposition: An Electrochemical in Situ X-Ray Diffraction Analysis. Journal of Physical Chemistry C, 2013, 117, 2688-2698.	3.1	12
99	Anodic behavior of mechanically alloyed Cu–Ni–Fe and Cu–Ni–Fe–O electrodes for aluminum electrolysis in low-temperature KF-AlF3 electrolyte. Electrochimica Acta, 2013, 112, 176-182.	5.2	32
100	Ultra high capacitance values of Pt@RuO2 core–shell nanotubular electrodes for microsupercapacitor applications. Journal of Power Sources, 2013, 221, 228-231.	7.8	36
101	Ruthenium Oxide Electrodeposition on Titanium Interdigitated Microarrays for Energy Storage. Materials Research Society Symposia Proceedings, 2013, 1494, 265-270.	0.1	Ο
102	Bismuth decoration of electrodeposited platinum thin films with a preferential (100) orientation. Materials Research Society Symposia Proceedings, 2013, 1491, 34.	0.1	0
103	Simultaneous Determination of the Permeability of a Nafion Membrane to Formic Acid and Water. Fuel Cells, 2013, 13, 1024-1031.	2.4	3
104	Ball-Milled (Cu-Ni-Fe + Fe ₂ O ₃) Composite as Inert Anode for Aluminum Electrolysis. Journal of the Electrochemical Society, 2013, 160, E55-E59.	2.9	12
105	3D-Percolating Model of Hydrous Ruthenium Oxide Dispersed in an Inert Polymer Matrix: An Impedance Spectroscopy Study. Journal of the Electrochemical Society, 2012, 159, F507-F513.	2.9	1
106	Mechanically Alloyed Cu-Ni-Fe-O Based Materials as Oxygen-Evolving Anodes for Aluminum Electrolysis. Journal of the Electrochemical Society, 2012, 159, E62-E68.	2.9	31
107	Investigation of cavity microelectrode technique for electrochemical study with manganese dioxides. Electrochimica Acta, 2012, 86, 268-276.	5.2	40
108	Structure and morphology of Pt3Sc alloy thin film prepared by pulsed laser deposition. Thin Solid Films, 2012, 524, 127-132.	1.8	7

#	Article	IF	CITATIONS
109	Metastable AuxRh100–x Thin Films Prepared by Pulsed Laser Deposition for the Electrooxidation of Methanol. Journal of Physical Chemistry C, 2012, 116, 5262-5269.	3.1	18
110	Effect of the nature of (100) surface sites on the electroactivity of macroscopic Pt electrodes for the electrooxidation of ammonia. Electrochemistry Communications, 2012, 22, 197-199.	4.7	43
111	Highly Porous and Preferentially Oriented {100} Platinum Nanowires and Thin Films. Advanced Functional Materials, 2012, 22, 4172-4181.	14.9	51
112	Preparation of PtAu Alloy Colloids by Laser Ablation in Solution and Their Characterization. Journal of Physical Chemistry C, 2012, 116, 13413-13420.	3.1	91
113	Effect of Al addition on the microstructure and low-temperature reactivity to oxygen of pre-formed MoSi2. Journal of Materials Science, 2012, 47, 6792-6800.	3.7	7
114	Synthesis and characterization of PtCo nanowires for the electro-oxidation of methanol. Journal of Power Sources, 2012, 206, 20-28.	7.8	35
115	Ball-Milled Cu-Ni-Fe-O Materials as Inert Anodes for Aluminum Electrolysis in Low-Temperature KF-AlF3 Electrolyte. , 2012, , 1377-1380.		0
116	Effect of Ball-Milling on the Physical and Electrochemical Properties of PbO ₂ and PbO ₂ /BaSO ₄ Nanocomposite. Journal of the Electrochemical Society, 2011, 159, A60-A67.	2.9	4
117	Influence of the iron content in Cu–Ni based inert anodes on their corrosion resistance for aluminium electrolysis. Corrosion Science, 2011, 53, 3248-3253.	6.6	35
118	PtCo 1D Nanostructures for Electrocatalytic Oxidation of Methanol. ECS Meeting Abstracts, 2011, , .	0.0	0
119	Carbon/PbO2 asymmetric electrochemical capacitor based on methanesulfonic acid electrolyte. Electrochimica Acta, 2011, 56, 8122-8128.	5.2	73
120	Synthesis of Cu–Pd alloy thin films by co-electrodeposition. Electrochimica Acta, 2011, 56, 7397-7403.	5.2	28
121	Comparative study on the structure and electrochemical hydriding properties of MgTi, Mg0.5Ni0.5Ti and MgTi0.5Ni0.5 alloys prepared by high energy ball milling. Journal of Power Sources, 2011, 196, 1561-1568.	7.8	23
122	Hydrazine oxidation at preferentially oriented Pt (100) nanowires array electrodes. Materials Research Society Symposia Proceedings, 2011, 1311, 10601.	0.1	1
123	Synthesis and Characterization of Well Aligned Ru Nanowires and Nanotubes. ECS Transactions, 2010, 25, 3-11.	0.5	20
124	Determination of the real surface area of powdered materials in cavity microelectrodes by electrochemical impedance spectroscopy. Electrochimica Acta, 2010, 55, 6283-6291.	5.2	46
125	Synthesis of fcc Mg–Ti–H alloys by high energy ball milling: Structure and electrochemical hydrogen storage properties. Journal of Power Sources, 2010, 195, 4370-4374.	7.8	29
126	Influence of the velocity of Pt ablated species on the structural and electrocatalytic properties of Pt thin films. International Journal of Hydrogen Energy, 2010, 35, 8486-8493.	7.1	9

#	Article	IF	CITATIONS
127	Influence of Pd on the structure and electrochemical hydrogen storage properties of Mg50Ti50 alloy prepared by ball milling. Electrochimica Acta, 2010, 55, 611-619.	5.2	26
128	Oxygen Reduction Kinetics on Pt[sub x]Ni[sub 100â^'x] Thin Films Prepared by Pulsed Laser Deposition. Journal of the Electrochemical Society, 2010, 157, B1051.	2.9	15
129	Effect of Size on the Electrochemical Stability of Pt Nanoparticles Deposited on Gold Substrate. Journal of Physical Chemistry C, 2010, 114, 2980-2988.	3.1	43
130	Structural and Electrochemical Characterization of Metastable PtAu Bulk and Surface Alloys Prepared by Crossed-Beam Pulsed Laser Deposition. Journal of Physical Chemistry C, 2010, 114, 2192-2199.	3.1	61
131	Structure and high-temperature oxidation behaviour of Cu–Ni–Fe alloys prepared by high-energy ball milling for application as inert anodes in aluminium electrolysis. Corrosion Science, 2010, 52, 3348-3355.	6.6	69
132	Influence of pressure on the Pt nanoparticle growth modes during pulsed laser ablation. Journal of Applied Physics, 2010, 108, .	2.5	43
133	Structural and Electrochemical Properties of Nanocrystalline PtRu Alloys Prepared by Crossed-Beam Pulsed Laser Deposition. Journal of Physical Chemistry C, 2010, 114, 18931-18939.	3.1	11
134	Electrolytic Production of Aluminum Using Mechanically Alloyed Cu–Al–Ni–Fe-Based Materials as Inert Anodes. Journal of the Electrochemical Society, 2010, 157, E173.	2.9	27
135	Electrodeposition of Arrays of Ru, Pt, and PtRu Alloy 1D Metallic Nanostructures. Journal of the Electrochemical Society, 2010, 157, K59.	2.9	30
136	Electrochemical Template Synthesis of Ordered Lead Dioxide Nanowires. Journal of the Electrochemical Society, 2009, 156, A645.	2.9	42
137	Microelectrode Study of Pore Size, Ion Size, and Solvent Effects on the Charge/Discharge Behavior of Microporous Carbons for Electrical Double-Layer Capacitors. Journal of the Electrochemical Society, 2009, 156, A7.	2.9	231
138	Structural and Electrochemical Hydriding Characteristics of Mg–Ti-Based Alloys Prepared by High Energy Ballmilling. Journal of the Electrochemical Society, 2009, 156, A967.	2.9	21
139	Synthesis of Ordered Lead Dioxide Nanowires using an Electroplating Template Method. ECS Transactions, 2009, 16, 207-211.	0.5	5
140	Effect of Ball-milling on the Physical and Electrochemical Properties of Lead Dioxide. ECS Transactions, 2009, 16, 213-220.	0.5	4
141	Synthesis and properties of novel benzimidazole-containing sulfonated polyethersulfones for fuel cell applications. Journal of Polymer Science Part A, 2009, 47, 1920-1929.	2.3	39
142	Ionomers for proton exchange membrane fuel cells by sulfonation of novel dendritic multiblock copoly(etherâ€sulfone)s. Journal of Polymer Science Part A, 2009, 47, 5461-5473.	2.3	26
143	Effect of the nanostructure on the CO poisoning rate of platinum. Electrochemistry Communications, 2009, 11, 834-837.	4.7	22
144	Enhanced stability and activity of PtRu nanotubes for methanol electrooxidation. Electrochemistry Communications, 2009, 11, 1449-1452.	4.7	30

#	Article	IF	CITATIONS
145	EQCM study of electrodeposited PbO2: Investigation of the gel formation and discharge mechanisms. Electrochimica Acta, 2009, 54, 7382-7388.	5.2	32
146	Synthesis and characterization of preferentially oriented (100) Pt nanowires. Electrochemistry Communications, 2009, 11, 1924-1927.	4.7	45
147	Design and synthesis of dipeptidyl nitriles as potent, selective, and reversible inhibitors of cathepsin C. Bioorganic and Medicinal Chemistry Letters, 2009, 19, 5392-5396.	2.2	36
148	Hydrogen Absorption in Nanocrystalline Cubic Ti-Based Compounds. Journal of Physical Chemistry C, 2009, 113, 1196-1203.	3.1	0
149	Structure and Electrochemical Hydrogen Storage Properties of Mg-Ti Based Materials Prepared by Mechanical Alloying. ECS Transactions, 2009, 16, 91-100.	0.5	12
150	Pt-Ru catalysts prepared by high energy ball-milling for PEMFC and DMFC: Influence of the synthesis conditions. Electrochimica Acta, 2008, 53, 5142-5154.	5.2	12
151	Laserâ€Fabricated Porous Alumina Membranes for the Preparation of Metal Nanodot Arrays. Small, 2008, 4, 572-576.	10.0	39
152	lonomers for proton exchange membrane fuel cells with sulfonic acid groups on the endâ€groups: Novel branched poly(etherâ€ketone)s with 3,6â€ditritylâ€9 <i>H</i> arbazole endâ€groups. Journal of Polymer Science Part A, 2008, 46, 3860-3868.	2.3	61
153	Structure and electrochemical behaviour of metastable Mg50Ti50 alloy prepared by ball milling. Journal of Power Sources, 2008, 175, 621-624.	7.8	59
154	Concept for Charge Storage in Electrochemical Capacitors with Functionalized Carbon Electrodes. Electrochemical and Solid-State Letters, 2008, 11, A202.	2.2	24
155	Studies of Nafion–RuO[sub 2]â‹xH[sub 2]O Composite Membranes. Journal of the Electrochemical Society, 2008, 155, B70.	2.9	11
156	Physico-Chemical and Electrochemical Properties of Platinumâ^'Tin Nanoparticles Synthesized by Pulsed Laser Ablation for Ethanol Oxidation. Journal of Physical Chemistry C, 2008, 112, 14672-14681.	3.1	34
157	Ionomers for Proton Exchange Membrane Fuel Cells with Sulfonic Acid Groups on the End Groups: Novel Branched Poly(etherâ [~] ketone)s. Macromolecules, 2008, 41, 281-284.	4.8	148
158	Ionomers for Proton Exchange Membrane Fuel Cells with Sulfonic Acid Groups on the End Groups: Novel Linear Aromatic Poly(sulfideâ^'ketone)s. Macromolecules, 2008, 41, 277-280.	4.8	93
159	In Vivo Inhibition of Serine Protease Processing Requires a High Fractional Inhibition of Cathepsin C. Molecular Pharmacology, 2008, 73, 1857-1865.	2.3	55
160	Inhibition of the Activation of Multiple Serine Proteases with a Cathepsin C Inhibitor Requires Sustained Exposure to Prevent Pro-enzyme Processing*. Journal of Biological Chemistry, 2007, 282, 20836-20846.	3.4	67
161	Electro-oxidation of Ethanol at Sputter-Deposited Platinum–Tin Catalysts. Journal of the Electrochemical Society, 2007, 154, B876.	2.9	34
162	Ethanol Electrooxidation on Pt-Sn Catalysts Deposited by Pulsed Laser Ablation. ECS Transactions, 2007, 6, 217-223.	0.5	0

#	Article	IF	CITATIONS
163	Functionally Modified Macroporous Membrane Prepared by using Pulsed Laser Deposition. Advanced Functional Materials, 2007, 17, 443-450.	14.9	28
164	Effect of boron on the structural and electrochemical properties of nanocrystalline Ti2RuFeBx electrodes. Electrochimica Acta, 2007, 52, 4497-4505.	5.2	0
165	Influence of an inert background gas on bimetallic cross-beam pulsed laser deposition. Journal of Applied Physics, 2006, 99, 034904.	2.5	55
166	Gold oxide thin film grown by pulsed laser deposition in an O2 atmosphere. Thin Solid Films, 2005, 472, 49-57.	1.8	54
167	Surface modification of co-evaporated thin films upon oxygen and air exposure. Surface Science, 2005, 595, 73-86.	1.9	3
168	Effect of Chromium Additives to Nanocrystalline Ti:Ru:Fe:O on the Reduction of Hypochlorite. Journal of the Electrochemical Society, 2005, 152, E265.	2.9	1
169	In Situ Spatial and Time-Resolved Studies of Electrochemical Reactions by Scanning Transmission X-ray Microscopy. Analytical Chemistry, 2005, 77, 3479-3487.	6.5	66
170	Modification to the composition of nanocrystalline RuO2 through reactive milling under O2. Journal of Alloys and Compounds, 2005, 400, 257-264.	5.5	11
171	Physicochemical Characterization of Mixed RuO2â^'SnO2 Solid Solutions. Chemistry of Materials, 2005, 17, 1570-1579.	6.7	140
172	Nanostructured Gold Thin Films Prepared by Pulsed Laser Deposition. Journal of Materials Research, 2004, 19, 950-958.	2.6	33
173	RBS and XRD analyses of carbon-coated stainless steel plates. Surface and Coatings Technology, 2004, 183, 216-223.	4.8	1
174	Activation and hydrogen absorption in thermally prepared RuO2 and IrO2. Journal of Electroanalytical Chemistry, 2004, 570, 13-27.	3.8	41
175	Effect of Graphite on the Electrochemical Properties of Ballmilled RuO[sub 2]. Journal of the Electrochemical Society, 2004, 151, A1141.	2.9	4
176	Growth dynamics of pulsed laser deposited Pt nanoparticles on highly oriented pyrolitic graphite substrates. Physical Review B, 2004, 70, .	3.2	73
177	Hydrogen production and crystal structure of ball-milled MgH2–Ca and MgH2–CaH2 mixtures. Journal of Alloys and Compounds, 2004, 376, 180-185.	5.5	76
178	Nanostructured Gold Thin Films Prepared by Pulsed Laser Deposition. Journal of Materials Research, 2004, 19, 950-958.	2.6	1
179	XPS investigations of thermally prepared RuO2 electrodes in reductive conditions. Electrochimica Acta, 2003, 48, 4245-4252.	5.2	175
180	Influence of the expansion dynamics of laser-produced gold plasmas on thin film structure grown in various atmospheres. Journal of Applied Physics, 2003, 94, 4796.	2.5	67

#	Article	IF	CITATIONS
181	Platinum nanoparticles growth by means of pulsed laser ablation. Materials Research Society Symposia Proceedings, 2003, 789, 91.	0.1	0
182	PEMFC Anode with Very Low Pt Loadings Using Pulsed Laser Deposition. Electrochemical and Solid-State Letters, 2003, 6, A125.	2.2	34
183	New Materials and Procedures to Protect Metallic PEM Fuel Cell Bipolar Plates. Journal of the Electrochemical Society, 2002, 149, A905.	2.9	52
184	Hydrogen Absorption in Thermally Prepared RuO[sub 2] Electrode. Electrochemical and Solid-State Letters, 2002, 5, E40.	2.2	24
185	Electrochemical Properties of Ruthenium-Based Nanocrystalline Materials as Electrodes for Supercapacitors. Chemistry of Materials, 2002, 14, 1210-1215.	6.7	142
186	Correlation between plasma expansion dynamics and gold-thin film structure during pulsed-laser deposition. Applied Physics Letters, 2002, 80, 1716-1718.	3.3	50
187	Plasma-sprayed nanocrystalline Ti–Ru–Fe–O coatings for the electrocatalysis of hydrogen evolution reaction. Journal of Alloys and Compounds, 2002, 345, 228-237.	5.5	9
188	X-ray photoelectron spectroscopy studies of the electrochemically n-doped state of a conducting polymer. Synthetic Metals, 2002, 132, 71-79.	3.9	21
189	Reactivity during cycling of nanocrystalline Mg-based hydrogen storage compounds. International Journal of Hydrogen Energy, 2002, 27, 909-913.	7.1	44
190	Preparation and corrosion behavior of nanocrystalline iron gradient materials produced by powder processing. Journal of Materials Processing Technology, 2002, 121, 383-389.	6.3	22
191	Activation characteristics of graphite modified hydrogen absorbing materials. Journal of Alloys and Compounds, 2001, 325, 245-251.	5.5	98
192	Study of the activation process of Mg-based hydrogen storage materials modified by graphite and other carbonaceous compounds. Journal of Materials Research, 2001, 16, 2893-2905.	2.6	72
193	Hybrid Nafion®-inorganic membrane with potential applications for polymer electrolyte fuel cells. Journal of Electroanalytical Chemistry, 2000, 489, 101-105.	3.8	107
194	Hydrogen electrosorption in nanocrystalline Ti-based alloys. Journal of Electroanalytical Chemistry, 2000, 480, 64-73.	3.8	12
195	XPS surface study of nanocrystalline Ti–Ru–Fe materials. Applied Surface Science, 2000, 158, 252-262.	6.1	43
196	Title is missing!. Journal of Applied Electrochemistry, 2000, 30, 491-498.	2.9	6
197	Title is missing!. Journal of Applied Electrochemistry, 2000, 30, 1243-1253.	2.9	31
198	High Energy Ballmilled Pt-Mo Catalysts for Polymer Electrolyte Fuel Cells and Their Tolerance to CO. Journal of the Electrochemical Society, 2000, 147, 3989.	2.9	25

#	Article	IF	CITATIONS
199	Effect of carbon-containing compounds on the hydriding behavior of nanocrystalline Mg2Ni. Journal of Alloys and Compounds, 2000, 307, 226-233.	5.5	49
200	Hydriding behavior of Mg–Al and leached Mg–Al compounds prepared by high-energy ball-milling. Journal of Alloys and Compounds, 2000, 297, 282-293.	5.5	165
201	Raney Type Surfaces Prepared by High Energy Ball Milling: Application to the Synthesis of Electroanalysts for the Sodium Chlorate Industry. Materials Science Forum, 1999, 312-314, 513-520.	0.3	1
202	Title is missing!. Journal of Applied Electrochemistry, 1999, 29, 951-960.	2.9	46
203	Kinetics of formation of nanocrystalline phases by mechanochemical reaction between Ti and RuO2. Journal of Materials Science, 1999, 34, 5581-5588.	3.7	6
204	Large specific surface area nanocrystalline Ti–Ru–Fe cathode materials for sodium chlorate. Journal of Applied Electrochemistry, 1999, 29, 627-635.	2.9	4
205	Title is missing!. Journal of Applied Electrochemistry, 1999, 29, 551-560.	2.9	14
206	Structural and surface characterizations of nanocrystalline Pt–Ru alloys prepared by high-energy ball-milling. Journal of Alloys and Compounds, 1999, 292, 301-310.	5.5	33
207	Effect of the Pre-Treatment of Carbon Black Supports on the Activity of Fe-Based Electrocatalysts for the Reduction of Oxygen. Journal of Physical Chemistry B, 1999, 103, 2042-2049.	2.6	188
208	Neutron and in Situ X-ray Investigation of Hydrogen Intake in Titanium-Based Cubic Alloys. Chemistry of Materials, 1999, 11, 3220-3226.	6.7	10
209	Iron catalysts prepared by high-temperature pyrolysis of tetraphenylporphyrins adsorbed on carbon black for oxygen reduction in polymer electrolyte fuel cells. Electrochimica Acta, 1998, 43, 341-353.	5.2	129
210	Activation and characterization of Fe-based catalysts for the reduction of oxygen in polymer electrolyte fuel cells. Electrochimica Acta, 1998, 43, 1969-1984.	5.2	100
211	Electrochemical behavior of nanocrystalline Ti2RuFe alloy prepared by high energy ball-milling. Journal of Electroanalytical Chemistry, 1998, 455, 83-92.	3.8	10
212	Effect of oxygen on the structural and electrochemical properties of nanocrystalline Ti-Ru-Fe alloy prepared by mechanical alloying. Scripta Materialia, 1998, 10, 523-541.	0.5	13
213	Increase of specific surface area of metal hydrides by lixiviation. Journal of Alloys and Compounds, 1998, 266, 307-310.	5.5	27
214	Influence of Nitrogenâ€Containing Precursors on the Electrocatalytic Activity of Heatâ€Treated Fe ( â€ on Carbon Black for  O 2 Reduction. Journal of the Electrochemical Society, 1998, 145, 2411-2418.	‰0Ha€% 2.9	‰â€‰) 2 102) 2
215	X-ray and Neutron Diffraction Study of Nanocrystalline Tiâ^'Ruâ^'Feâ^'O Compounds. Chemistry of Materials, 1998, 10, 3492-3497.	6.7	13

²¹⁶Comparative Study of the Electrochemical Behavior of Polycrystalline and Nanocrystalline Ru
Powder in NaOH Solution. Journal of the Electrochemical Society, 1998, 145, 1624-1631.2.915

#	Article	IF	CITATIONS
217	Structural and electrochemical properties of Ti–Ru–Fe–O alloys prepared by high energy ball-milling. Journal of Materials Research, 1998, 13, 1171-1176.	2.6	14
218	Metastable Ti-Ru-Fe-O Nanocrystalline Alloys for the Hydrogen Evolution Reaction in the Chlorate Industry. Materials Science Forum, 1997, 235-238, 979-984.	0.3	3
219	Activation of Ruthenium Oxide, Iridium Oxide, and Mixed RuxIr1 â^ x Oxide Electrodes during Cathodic Polarization and Hydrogen Evolution. Journal of the Electrochemical Society, 1997, 144, 573-581.	2.9	89
220	High energy ball-milled Ti2RuFe electrocatalyst for hydrogen evolution in the chlorate industry. Journal of Materials Research, 1997, 12, 1492-1500.	2.6	24
221	Highâ€Performance, Low Pt Content Catalysts for the Electroreduction of Oxygen in Polymerâ€Electrolyte Fuel Cells. Journal of the Electrochemical Society, 1997, 144, 145-154.	2.9	77
222	Activation of Various Feâ€Based Precursors on Carbon Black and Graphite Supports to Obtain Catalysts for the Reduction of Oxygen in Fuel Cells. Journal of the Electrochemical Society, 1997, 144, 218-226.	2.9	86
223	Electroreduction of Oxygen in Polymer Electrolyte Fuel Cells by Activated Carbon Coated Cobalt Nanocrystallites Produced by Electric Arc Discharge. Chemistry of Materials, 1997, 9, 784-790.	6.7	29
224	Is nitrogen important in the formulation of Fe-based catalysts for oxygen reduction in solid polymer fuel cells?. Electrochimica Acta, 1997, 42, 1379-1388.	5.2	207
225	Metastable Ti-Ru-Fe-O nanocrystalline alloys for applications in the chlorate industry. Materials Science & Engineering A: Structural Materials: Properties, Microstructure and Processing, 1997, 226-228, 915-919.	5.6	3
226	AFM observation of surface activation of ruthenium oxide electrodes during hydrogen evolution. Journal of Electroanalytical Chemistry, 1997, 429, 185-192.	3.8	21
227	Intercalation of CoCl2 into graphite: Mixing method vs molten salt method. Carbon, 1997, 35, 299-306.	10.3	8
228	Low Overpotential Nanocrystalline Ti-Fe-Ru-O Cathodes for the Production of Sodium Chlorate. Materials Science Forum, 1996, 225-227, 795-800.	0.3	11
229	New class of potent ligands for the human peripheral cannabinoid receptor. Bioorganic and Medicinal Chemistry Letters, 1996, 6, 2263-2268.	2.2	86
230	Heat-treated iron and cobalt tetraphenylporphyrins adsorbed on carbon black: Physical characterization and catalytic properties of these materials for the reduction of oxygen in polymer electrolyte fuel cells. Electrochimica Acta, 1996, 41, 1689-1701.	5.2	243
231	Carbon monoxide poisoning of platinum-graphite catalysts for polymer electrolyte fuel cells: comparison between platinum-supported on graphite and intercalated in graphite. Journal of Power Sources, 1996, 61, 193-200.	7.8	14
232	Catalytic activity and stability of heat-treated iron phthalocyanines for the electroreduction of oxygen in polymer electrolyte fuel cells. Journal of Power Sources, 1996, 61, 227-237.	7.8	150
233	Electrocatalytic Properties of Nanocrystalline Alloys: Effect of the Oxygen Concentration in Ti ₂ RuFeO _x Alloy on the Structural and Electrochemical Properties. Materials Science Forum, 1996, 225-227, 801-806.	0.3	7
234	Crystallite Size Effects of Carbonâ€Supported Platinum on Oxygen Reduction in Liquid Acids. Journal of the Electrochemical Society, 1996, 143, 18-23.	2.9	107

#	Article	IF	CITATIONS
235	Kinetics of the Hydrogen Evolution Reaction on RuO2 and IrO2 Oxide Electrodes in  H 2 SO 4 So An AC Impedance Study. Journal of the Electrochemical Society, 1996, 143, 3576-3584.	olution:	56
236	Hydrogen Evolution Reaction in Alkaline Solution: Catalytic Influence of Pt Supported on Graphite vs. Pt Inclusions in Graphite. Journal of the Electrochemical Society, 1996, 143, 919-926.	2.9	35
237	Physical, chemical and electrochemical characterization of heat-treated tetracarboxylic cobalt phthalocyanine adsorbed on carbon black as electrocatalyst for oxygen reduction in polymer electrolyte fuel cells. Electrochimica Acta, 1995, 40, 2635-2646.	5.2	173
238	Preparation and chemical reduction of Pt(IV) chloride-GICS: Supported Pt vs Pt inclusion graphite compounds. Carbon, 1995, 33, 1265-1278.	10.3	14
239	Surface characterization by time-of-flight SIMS of a catalyst for oxygen electroreduction: pyrolyzed cobalt phthalocyanine-on-carbon black. Applied Surface Science, 1995, 84, 9-21.	6.1	58
240	AFM and XPS characterization of the Si(111) surface after thermal treatment. Applied Surface Science, 1995, 90, 481-487.	6.1	4
241	Composition and thermal-annealing-induced short-range ordering changes in amorphous hydrogenated silicon carbide films as investigated by extended x-ray-absorption fine structure and infrared absorption. Physical Review B, 1995, 51, 4903-4914.	3.2	23
242	Morphological Evolution of Chloroaluminum Phthalocyanine Thin Films Followed in situ by Atomic Force Microscopy. The Journal of Physical Chemistry, 1995, 99, 17198-17206.	2.9	14
243	Influence of Loading on the Activity and Stability of Heatâ€Treated Carbonâ€Supported Cobalt Phthalocyanine Electrocatalysts in Solid Polymer Electrolyte Fuel Cells. Journal of the Electrochemical Society, 1995, 142, 1162-1168.	2.9	49
244	Oxidation of Si(1?1?1) promoted by K multilayers: K and SiO2 islands. Applied Physics A: Materials Science and Processing, 1995, 61, 187-191.	2.3	0
245	Activation of the human peripheral cannabinoid receptor results in inhibition of adenylyl cyclase. Molecular Pharmacology, 1995, 48, 352-61.	2.3	128
246	Electrocatalytic Activity of Nafionâ€Impregnated Pyrolyzed Cobalt Phthalocyanine: A Correlative Study Between Rotating Disk and Solid Polymer Electrolyte Fuel ell Electrodes. Journal of the Electrochemical Society, 1994, 141, 41-45.	2.9	59
247	Graphitization and particle size analysis of pyrolyzed cobalt phthalocyanine/carbon catalysts for oxygen reduction in fuel cells. Journal of Materials Research, 1994, 9, 3203-3209.	2.6	54
248	Selected Dissolution of Aluminum Initiated by Atomic Force Microscope Tipâ€Surface Interaction. Journal of the Electrochemical Society, 1994, 141, L43-L45.	2.9	19
249	Atomic force microscopy study of the microroughness of SiC thin films. Thin Solid Films, 1994, 249, 38-43.	1.8	6
250	Chemical Bonding in Restacked Single-Layer MoS2 by X-ray Absorption Spectroscopy. Chemistry of Materials, 1994, 6, 614-619.	6.7	38
251	Characterization of New Systems for the Catalytic Electroreduction of Oxygen by Electrochemistry and X-Ray Absorption Spectroscopy. , 1994, , 281-293.		0
252	Partial oxidation of methane over ruthenium catalysts. Catalysis Letters, 1993, 21, 99-111.	2.6	42

#	Article	IF	CITATIONS
253	Pyrolyzed Cobalt Phthalocyanine as Electrocatalyst for Oxygen Reduction. Journal of the Electrochemical Society, 1993, 140, 1974-1981.	2.9	131
254	Physicochemical characteristics of electrochemically deposited molybdenum sulfide and polypyrrole-tetrathiomolybdate/molybdenum trisulfide composite electrodes. Chemistry of Materials, 1993, 5, 861-868.	6.7	39
255	Iron atomic packing in Fe-Ru superlattices by x-ray-absorption spectroscopy. Physical Review B, 1993, 47, 2344-2352.	3.2	23
256	Two timeâ€dependent, focusâ€dependent experiments using the energyâ€dispersive spectrometer at LURE. Review of Scientific Instruments, 1992, 63, 960-965.	1.3	10
257	Anisotropy of the core-hole relaxation in x-ray-absorption spectroscopy as probed in square planar cuprates. Physical Review B, 1992, 45, 8091-8096.	3.2	46
258	Origin of the electrocatalytic properties for oxygen reduction of some heat-treated polyacrylonitrile and phthalocyanine cobalt compounds adsorbed on carbon black as probed by electrochemistry and x-ray absorption spectroscopy. The Journal of Physical Chemistry, 1992, 96, 10898-10905.	2.9	152
259	In situ x-ray absorption spectroscopy study of underpotential deposition of copper on platinum (100). Electrochimica Acta, 1992, 37, 1977-1982.	5.2	28
260	In-situ time-resolved EXAFS study of the structural modifications occurring in nickel oxide electrodes between their fully oxidized and reduced states. Journal of Electroanalytical Chemistry and Interfacial Electrochemistry, 1991, 305, 83-95.	0.1	16
261	Structural and electronic characterization of underpotentially deposited copper on gold single crystal probed by in situ X-ray absorption spectroscopy. Electrochimica Acta, 1991, 36, 1859-1862.	5.2	44
262	Electronic and structural characterization of underpotentially deposited submonolayers and monolayer of copper on gold (111) studied byin situx-ray-absorption spectroscopy. Physical Review Letters, 1991, 66, 2235-2238.	7.8	116
263	X-ray absorption spectroscopy: A fluorescence detection system based on a plastic scintillator. Nuclear Instruments and Methods in Physics Research, Section A: Accelerators, Spectrometers, Detectors and Associated Equipment, 1990, 294, 382-390.	1.6	17
264	In-plane structural and electronic characteristics of underpotentially deposited copper on gold (100) probed by in-situ X-ray absorption spectroscopy. Journal of Electroanalytical Chemistry and Interfacial Electrochemistry, 1990, 289, 263-278.	0.1	70
265	Electrochemical inclusion of copper and iron species in a conducting polymer observed in situ using time-resolved X-ray absorption spectroscopy. Faraday Discussions of the Chemical Society, 1990, 89, 41.	2.2	10
266	Characterization of metal/organic molecule and metal/polymer interfaces by NEXAFS spectroscopy. Faraday Discussions of the Chemical Society, 1990, 89, 275.	2.2	14
267	Investigation of aluminum phthalocyanine films by transmission electron microscopy. Journal of Materials Research, 1989, 4, 651-658.	2.6	13